Environmental Science and Pollution Research (2021) 28:33083–33095
https://doi.org/10.1007/s11356-021-13017-2

RESEARCH ARTICLE

Effects of fluoride emission on the morphoanatomy of three plant species endemics to Brazil using passive biomonitoring

Thamires Fernanda Gomes[1] · Ademir Martins Lima[2] · Ana Paula Pires Marques[1] · Luzimar Campos da Silva[1]

Received: 1 November 2020 / Accepted: 15 February 2021 / Published online: 26 February 2021

Abstract

Fluoride is the most phytotoxic atmospheric pollutant. The objective of this study was to evaluate the effects of fluoride emissions by an aluminum smelter on three plant species endemics to Brazil, located at Parque Estadual do Itacolomi (PEI). The monitored species were *Byrsonima variabilis* (Malpighiaceae), *Myrceugenia alpigena* (Myrtaceae), and *Eremanthus erythropappus* (Asteraceae), which were monitored during 9 months using passive biomonitoring at five different locations with different distances from the smelter. The monitored species did not show macroscopic phytotoxicity damage to fluoride; however, they did show microscopic damage. The species closer to the smelter presented more severe anatomic damages, such as rupture of cell walls, protoplast retraction, and trichome alterations. Damaged stomatal ledges, flaking epicuticular wax, and damages to trichomes were observed. *M. alpigena* showed a higher accumulation of fluoride than the other species at all monitored sites. The test for cell death with Evans Blue was positive for the three studied species. Through biomonitoring in the PEI, we concluded that the emissions from the aluminum smelter affect the native vegetation and that due to the greater accumulation of fluoride and the diversity of microscopic damage in *M. alpigena*, the use of this species in the monitoring of environments polluted by fluoride is enhanced.

Keywords *Myrceugenia alpigena* · *Byrsonima variabilis* · *Eremanthus erythropappus* · Atmospheric pollution · Anatomical alteration · Evans Blue · Endemic plants

Introduction

The constant progress of industrialization and urbanization has increased the incidence of pollutant emissions to the atmosphere. These pollutants, when in high concentrations, pose a threat to humans and the environment as a whole (Davison and Weinstein 2006; Yepu et al. 2017; Li et al. 2018; Mukherjee et al. 2019).

Fluoride is an air pollutant, emitted mainly in the form of hydrogen fluoride (HF). This process takes place through anthropogenic sources such as aluminum smelting, glass and ceramic manufacturing, mineral fertilizers production, and dental products, among others (Weinstein and Davison 2004; Ahmad et al. 2012; Hong et al. 2018; Ron Fuge 2019).

Fluorine belongs to the halogen family; it has strong electronegativity and reactive characteristics (Fordyce et al. 2007; Panda 2015). Thus, this element can cause damage to vegetation even at extremely low concentrations in the atmosphere, being considered, among the various air pollutants, the most phytotoxic (Klumpp et al. 1996; Weinstein and Davison 2003; Panda 2015).

Fluoride in aqueous solution can be absorbed over the entire leaf surface through the cuticle. In its gaseous state, this pollutant is absorbed through leaf stomata, which is the main route of fluoride absorption by plants. Inside the leaf, fluoride moves via apoplast, through the transpiratory current, to the leaves' margins and apices, which can cause injuries in these places. Fluoride can also accumulate in the mesophyll and can cause various damages, such as cell collapse (Weinstein and Davison 2004; Baunthiyal and Ranghar 2014; Anjos et al. 2018; Sharma and Kaur 2018). Plants contaminated by fluoride may show macroscopic changes such as leaf chlorosis, which is attributed to the collapse of chloroplasts and

Responsible Editor: Gangrong Shi

✉ Luzimar Campos da Silva
luzimar@ufv.br

[1] Departamento de Biologia Vegetal, Universidade Federal de Viçosa, Av. P.H. Rolfs, s/n, Campus Universitário, Vicosa, MG 36570-900, Brazil

[2] Departamento de Agronomia, Universidade Federal de Viçosa, Av. P.H. Rolfs, s/n, Campus Universitário, Vicosa, MG 36570-900, Brazil

disturbances in pigment synthesis (Fornasiero 2003; Louback et al. 2016; Anjos et al. 2018; Rodrigues et al. 2018a, 2020a, 2020b). Microscopic changes such as cuticle and trichome rupture, epicuticular wax flaking, and damage to stomatal ridges (Fornasiero 2001; Sant'Anna-Santos et al. 2012; Louback et al. 2016; Anjos et al. 2018), in addition to cellular changes and cell collapse (Silva et al. 2000; Sant'Anna-Santos et al. 2014, 2019; Rodrigues et al. 2017, 2018a, 2020a), have been reported.

Biomonitoring systematically uses responses from living organisms to assess changes in the environment, usually caused by anthropogenic actions (Matthews et al. 1982; Gorelova and Frontasyeva 2017; Yalaltdinova et al. 2018). This method is suitable for monitoring the long-term impact of fluoride emissions on vegetation close to sources of this pollutant, besides being a more economical method than the use of analytical instruments (Weinstein et al. 1990; Temmerman et al. 2004). In passive biomonitoring, experiments are carried out with plants evaluated at their natural place of occurrence (Gupta and Kulshrestha 2016).

The bioindicator potential of some plants or their mechanisms of tolerance in the face of air pollution have been studied since the 1980s, through morphophysiological and biochemical changes (Koslowski 1980). In the following decade, the European Union launched EuroBionet, an air quality assessment program using bioindicator plants (Klumpp et al. 2001). The program used mainly herbaceous species, and, until today, there are few studies that have reported the responses of tropical arboreal plants exposed to air pollutants (Silva et al. 2000; Sant'Anna-Santos et al. 2007; Rodrigues et al. 2017, 2018b; Anjos et al. 2018).

The state of Minas Gerais produces more than 135,000 tons of primary aluminum per year and is one of the largest aluminum producers in Brazil (ABAL 2011). In the city of Ouro Preto, there is an aluminum smelter installed, an emitting source of atmospheric fluoride (Weinstein and Davison 2004; Divan Junior et al. 2008; Louback et al. 2016). Between 2000 and 2002, the atmospheric concentration of fluoride in an air monitoring station located in the city center of Ouro Preto showed daily minimum values between 0.10 and 0.15 μg m^{-3} and daily maximum values between 6.22 and 12.87 μg m^{-3} (Assis et al. 2003). Some studies have been carried out in this region in order to observe the damage caused by fluoride in the vegetation, either through passive biomonitoring (Divan Junior et al. 2008), analyzing plants present in the vicinity of the polluting source, or through plants that were exposed in the desired locations, using active biomonitoring (Sant'Anna-Santos and Azevedo 2010; Louback et al. 2016).

The Parque Estadual do Itacolomi (PEI) consists of an ecosystem known as "rocky fields" (Campos Rupestres), and it has particular ecological conditions, with a large number of endemic species (Romero and Nakajima 1999). The PEI is located near the aluminum smelter in the city of Ouro Preto. In a study carried out at four sites within the PEI, through active biomonitoring, the contamination of individuals from *Spondias dulcis* exposed in these places was verified (Louback et al. 2016). However, natural species from this ecosystem have not yet been monitored.

In Brazil, few studies have addressed the effects caused by fluoride on the tropical ecosystem and on native vegetation (Weinstein and Hansen 1988; Arndt et al. 1995; Klumpp et al. 1996, 1998; Silva et al. 2000; Oliva et al. 2005; Divan Junior et al. 2007, 2008), this study being the first where native species from "rocky fields" (Campos Rupestres) and endemic to Brazil have been monitored through passive biomonitoring. The monitored species were *Eremanthus erythropappus* (Asteraceae), *Byrsonima variabilis* (Malpighiaceae), and *Myrceugenia alpigena* (Myrtaceae), where there are no studies in the scientific literature involving the effects of fluoride on the last two species. Thus, this study aims to evaluate the effect of emissions from an aluminum smelter on native species from the Parque Estadual do Itacolomi (PEI), in order to determine the sensitivity or tolerance of these species to fluoride. The hypothesis to be tested is that the fluoride released by the polluting source reaches the PEI vegetation, causing damage to the species in this park.

Materials and methods

Study area location

The passive biomonitoring was conducted at Parque Estadual do Itacolomi (PEI) (43° 32′ 30″–43° 22′ 30″ W; 20° 22′ 30″–20° 30′ 00″ S), in the city of Ouro Preto, Minas Gerais, Brazil. The PEI has an area of approximately 7000 ha, with a maximum altitude of 1772 m; it is located at the southern portion of Serra do Espinhaço Biosphere Reserve and southeast of the Quadrilátero Ferrífero, comprising a transition zone between Mata Atlântica and Cerrado (Peron 1989; Messias et al. 2017).

Botanical material and treatment

Individuals belonging to the following three species were monitored: *Myrceugenia alpigena* (DC.) Ladrum (Myrtaceae), *Byrsonima variabilis* (DC.) (Malpighiaceae), and *Eremanthus erythropappus* (DC.) MacLeisch (Asteraceae), all native from the PEI (Fig. 1). The species identities were confirmed by the specialists Marcos E. G. Sobral (Universidade Federal de São João Del-Rei, Departamento de Ciências Naturais), Maria C. H. Mamede (Instituto de Botânica, Centro de Pesquisa em Plantas Vasculares, Núcleo de Pesquisa da Curadoria do Herbário de São Paulo), and Eric K. O. Hattori (Universidade Federal dos Vales do Jequitinhonha e Mucuri, Instituto de Ciências

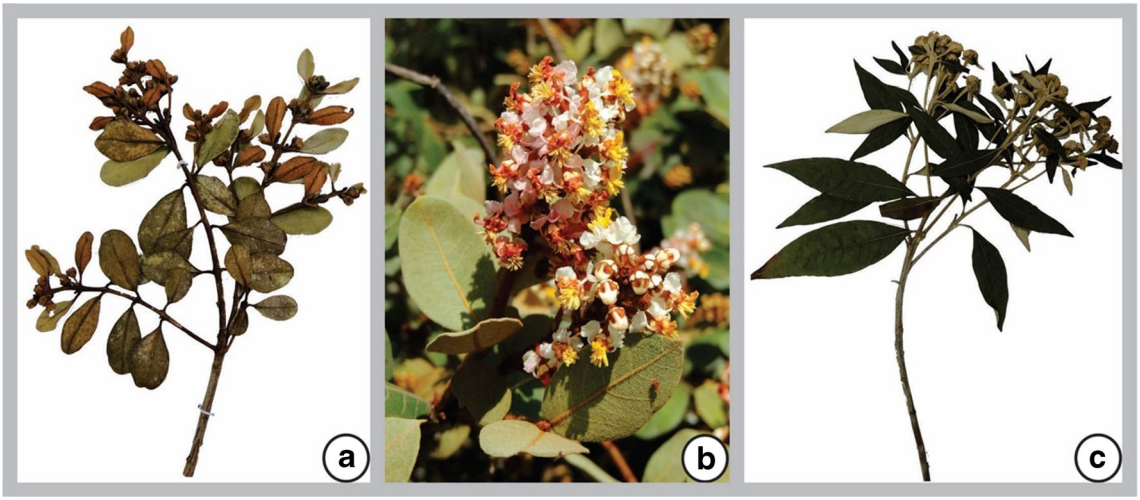

Fig. 1 Monitored species at Parque Estadual do Itacolomi (PEI). (A) *Myrceugenia alpigena.* (B) *Byrsonima variabilis.* (C) *Eremanthus erythropappus*

Agrárias), respectively. The voucher specimens were deposited at the Herbarium VIC of the Universidade Federal de Viçosa under the numbers 43996 (*M. alpigena*), 43997 (*B. variabilis*), and 43998 (*E. erythropappus*).

The experiment consisted of a passive exposure of five individuals (n = 5) of each studied species present in the PEI, featuring a passive biomonitoring. Five locations were monitored at different distances from the fluoride emitting source, four of these within the PEI and one outside the PEI, closer to the smelter. The location of the PEI and the monitored sites are shown in Fig. 2. Since it was a study carried out in the field, it was not possible to register the presence of all studied species in all monitored sites. The distribution of species per sampling site is shown in Table 1, in addition to the altitude and distance from the smelter of each site. The individuals were monitored for a period of 9 months, from April to December 2014.

Microenvironmental analyses

Microenvironmental analyses were carried out close to the individuals monitored at the PEI, from 9:00 to 12:00, between the months of April and December 2014. The determined parameters were altitude (m), temperature (°C), relative humidity (%), and wind speed (m s^{-1}), obtained using the Kestrel equipment (model 4300, Nielsen-Kellerman, USA).

Evaluation of visual symptoms

Three branches of each individual (n = 3) of each species were monitored at each site in the PEI. The leaves were photographed by a digital camera (model Cyber-Shot DSC-W310, Sony Corporation, Japan) to record any visual symptoms, such as chlorosis and necrosis caused by the smelter's emissions. To calculate the percentage of necrotic leaf area, a visual phytotoxicity classification scale was used: slightly injured (with sparse necrotic and chlorotic spots), moderately injured (from 30 to 50% of the leaf area necrotic), very injured (from 50 to 70% of the leaf area necrotic), and extremely injured (with more than 70% of the leaf area necrotic) (Silva et al. 2000).

Determination of fluoride content

Leaves from the individuals of all treatments were collected from the third node (from apical bud) and then oven-

Table 1 Altitude, distance from emitting source, and species distribution of each monitored site at Parque Estadual do Itacolomi (PEI-MG)

Sampling sites	Altitude (m)	Distance from emitting source (km)	Species		
			Myrceugenia alpigena	*Byrsonima variabilis*	*Eremanthus erythropappus*
Site 1	1278	3.83	–	X	X
Site 2	1508	4.33	–	X	X
Site 3	1542	2.38	X	X	X
Site 4	1140	1.62	X	X	X
Site 5	1077	0.78	–	X	–

– = missing species; X = present species

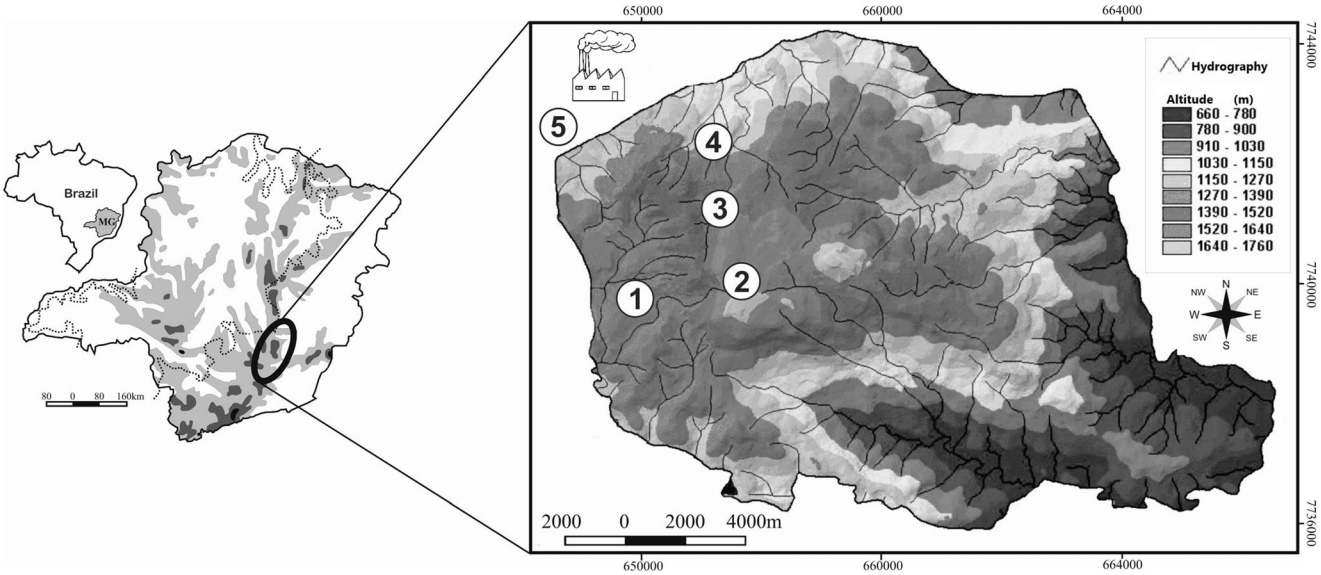

Fig. 2 Location of Parque Estadual do Itacolomi (PEI) and the sites where the species were monitored. Modified from Coser et al. (2010). (1, 2, 3, 4) Monitored sites within the PEI. (5) Monitored site in the PEI surroundings, posteriorly added due to a wildfire in the park

dried at 65 °C and reduced in a Wiley mill. Aliquots of 0.25 g were subjected to extraction in 0.5 M sulfuric acid (Fialho 1997). The fluoride potentiometric determination was performed using a selective ionic fluoride electrode (Thermo Scientific Fluoride Ions Selective Electrode, Massachusetts, USA) coupled to an ion analyzer device (Orion Research Incorporated EA 920, Massachusetts, EUA).

Anatomical analysis—light microscopy

For anatomical analysis, fully expanded leaves from the third node (from apical bud), containing no visual symptoms, were collected from the individuals at each monitoring site in the PEI. For anatomical studies, leaf samples were fixed in a solution of glutaraldehyde (2.5%) and paraformaldehyde (10%), in 0.1 M sodium phosphate buffer (pH 7.2), plus 5 mM calcium chloride (Karnovsky 1965). Subsequently, the material was dehydrated in a growing ethyl series and included in historesin glycol-methacrylate (Leica Historesin, Nussloch/Heidelberg, Germany), according to Gerrits (1964).

Transverse sections (4 μm thick) were obtained using an automated rotary microtome (model RM2265, Leica Microsystems Inc., Deerfield, USA) and stained in Toluidine blue (pH = 4.0) (O'Brien and McCully 1981). The permanent glass slides were mounted on Permount. All images were captured using a light microscope (model Olympus AX70TRF, Olympus Optical, Tokyo, Japan) with an image capture system (model Axio Vision Release 4.8.1, Carl Zeiss Vision GmbH, Germany).

Micromorphological analyses—scanning electron microscopy

For micromorphological analysis, samples without visual symptoms, collected from the third node (from apical bud), were fixed in Karnovsk solution in pH 7.2 sodium phosphate buffer (Karnovsky 1965). The samples were dehydrated in an ethyl series and dried to the critical point using the Critical Point Dryer equipment (CPD 030, Bal-Tec, Balzers, Liechtenstein). The leaf fragments were coated with gold in a metallizer (Sputter Coater model FDU010, Bal-Tec, Balzers, Liechtenstein).

The photographic documentation was performed using a scanning electron microscope (model 1430 VP, LEO, Cambridge, England) using the Iridium Ultra software. The equipment belongs to the Microscopy and Microanalysis Center, UFV.

Cell death detection

For the detection of cell death, samples from the median region of leaves without visual symptoms, located in the third node (from apical bud) in all species, were immersed in Evans Blue 0.1% solution for 40 min, immediately after collection. Then, the samples were clarified for 4 days in 95% alcohol at 65 °C (Kato et al. 2007). The glass slides were mounted in glycerin water and photographed under a light microscope (model Olympus AX70TRF, Olympus Optical, Tokyo, Japan) with an image capture system (model Axio Vision Release 4.8.1, Carl Zeiss Vision GmbH, Germany). In this test, the Evans Blue reagent only infiltrates cells with altered membrane permeability, a typical symptom of dead cells, staining them blue (Gaff and Okong'o-ogola 1971).

Statistical analysis

The experimental design was completely randomized, with five replications ($n = 5$). The data were submitted to analysis of variance (ANOVA), using the software Sisvar (Ferreira 2011). The treatment means were compared using the Tukey test, at 5% significance ($p < 0.05$).

Results

Microenvironmental analyses

According to the microenvironmental analyses, in December, there was a higher relative humidity than in the other evaluated months. The month with the highest temperature during the monitoring period was November. The months with the highest incidence of wind were July and November (Fig. 3).

Quantification of visual damage

The leaves of the monitored branches of each individual ($n = 3$), at all monitored sites in the PEI, did not show any visual symptoms (chlorosis and necrosis) during the monitoring period.

Determination of fluoride content

According to the quantification of fluoride in dry matter carried out in July 2014, among the three species monitored in the PEI, the individuals of *M. alpigena* had a higher fluoride content, followed by *B. variabilis* and *E. erythropappus* (Fig. 4A).

M. alpigena accumulated 25.2 μg g^{-1} of fluoride at site 3, and 22.6 μg g^{-1} at site 4, differing from the other species at these same sites, but not differing in the comparison between sites for the same species. Individuals of *M. alpigena* were found and monitored only at sites 3 and 4 (Fig. 4A).

B. variabilis showed fluoride levels of 8.5 and 9.2 μg g^{-1} at sites 1 and 2, and 12.5 and 13 μg g^{-1} at sites 3 and 4, respectively. Among the monitoring sites of this species, there was no significant difference in the fluoride content. *E. erythropappus* also did not differ statistically in the accumulation of fluoride between the monitoring sites. At sites 1, 2, 3, and 4, the individuals presented 7.8, 9.0, 9.0, and 10.1 μg g^{-1} of fluoride, respectively (Fig. 4A).

Sites 3 and 4 were the most representative of the sites monitored in July, where the species *M. alpigena* showed significant accumulation of fluoride.

In the quantification of fluoride performed in November 2014, *M. alpigena* showed a significant difference in the accumulation of this element when compared to the other monitored species, presenting 23 μg g^{-1} of this element in site 4, but not differing from the quantification carried out in July at the same site (Fig. 4B).

B. variabilis showed 13 μg g^{-1} of fluoride in individuals at site 4, not differing from the quantification carried out in July at the same site. At sites 1 and 2, the species showed 8 and 8.8 μg g^{-1} of fluoride, respectively. In addition to the sites at which *B. variabilis* was monitored within the PEI, individuals closest to the smelter were also collected in the PEI surroundings, at site 5. At this site, this species showed 13.2 μg g^{-1} of fluoride. There was no difference in the fluoride content in *B. variabilis* between the monitored sites and between the 2 months of collection (Fig. 4B).

E. erythropappus showed 8.5, 10.5, and 10.5 μg g^{-1} of fluoride at sites 1, 2, and 4, respectively. There was no significant difference between the sites sampled this month, nor was there any difference between the quantification performed in the months of July and November (Fig. 4B).

In November, it was not possible to collect material for quantification of fluoride from the individuals of site 3 due to a wildfire that occurred in the PEI, which resulted in the death of all individuals monitored at this site. In view of this problem, it was decided to add site 5 (close to the smelter) to the present work.

Anatomical and micromorphological analyses

The leaf of *Myrceugenia alpigena* is hypostomatic, presenting a uniseriate epidermis, with nonglandular trichomes. The mesophyll is dorsiventral, presenting secretory cavities close to the palisade parenchyma (Fig. 5A).

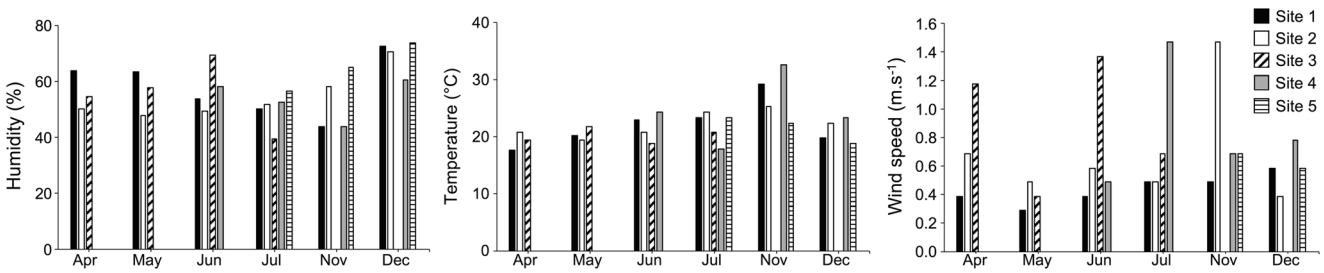

Fig. 3 Microenvironmental analyses at the different monitoring sites in the PEI, from April to December 2014. Humidity (%), temperature (°C) and wind speed ($m.s^{-1}$). Apr, April; Jun, June; Jul, July; Nov, November; Dec, December

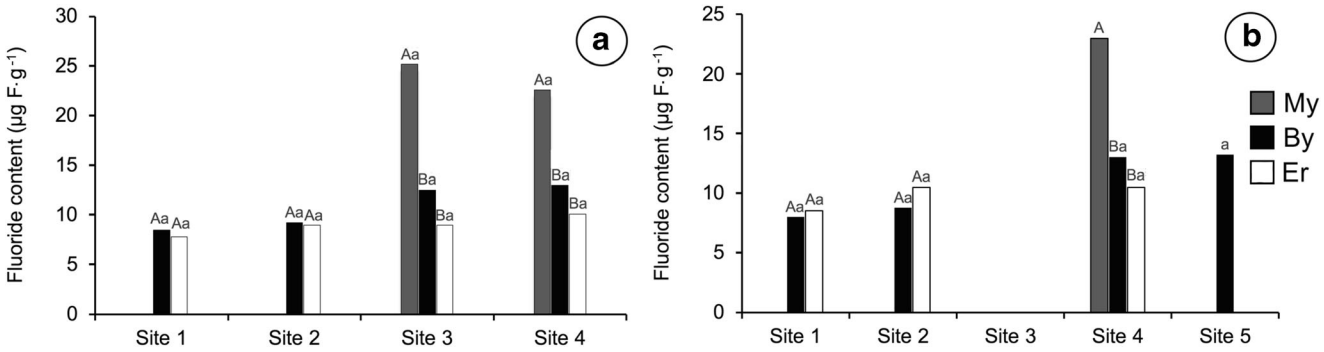

Fig. 4 Fluoride content (µg F.g^{-1}) in each species per monitored site. (A) Quantification performed in July 2014. (B) Quantification performed in November 2014. My, *Myrceugenia alpigena*; By, *Byrsonima variabilis*; Er, *Eremanthus erythropappus*. Uppercase letters compare different species at the same site. Lowercase letters compare the same species at different sites. Means followed by the same letter did not differ by Tukey's test, at 5% probability ($p < 0.05$)

At the two sites where *M. alpigena* was monitored (sites 3 and 4), anatomical damage was observed. At these sites, the individuals presented retraction of protoplasts and cells of the midrib collenchyma with an altered shape (Fig. 5B, C, D), in addition to deformation in the nonglandular trichomes (Fig. 5A).

From the observation with a scanning electron microscope (SEM), at the two sites (3 and 4) where the collection was performed, it was possible to observe the presence of flaccid trichomes in *M. alpigena* (Fig. 5E and F) and in some areas they were even lost, remaining only their bases (Fig. 5E and H). Stomata with damaged ledges (Fig. 5G and H) and furrows formation in the epidermis of these plants (Fig. 5E) were also observed.

Byrsonima variabilis presents hypostomatic leaf, with uniseriate epidermis and thick cuticle on both sides of the leaf. The stomata are located on the same level as the other epidermal cells and the guard cells have a prominent stomatal ledge; the mesophyll is isobilateral (Fig. 6A).

The leaves of the individuals at site 3 (Fig. 6C) presented cells of the parenchyma and collenchyma of the midrib with an altered shape. At sites 1, 4, and 5 (Fig. 6B, D, and E), the same modification was also observed in the monitored plants.

From the observation with SEM in *B. variabilis*, flaccid trichomes (Fig. 6F), epicuticular wax flaking, and damaged stomata, with rupture of the stomatal ledge (Fig. 6G and H), were observed in the individuals at sites 1 and 4.

The leaf blade of *Eremanthus erythropappus* is hypostomatic, with dorsiventral mesophyll. The epidermis is uniseriate, with a thin cuticle (Fig. 7A). Glandular trichomes were observed in the epidermis of both sides of the leaf (Fig. 7A and B), in addition to nonglandular trichomes, which were found on the leaf's abaxial surface (Fig. 7A).

In *E. erythropappus*, the individuals at sites 1 and 3 presented glandular trichomes apparently ruptured (Fig. 7B). Scanning electron microscopy showed changes in the glandular trichomes, which were ruptured (Fig. 6C, D, E, and F). In addition, there was a proliferation of fungal hyphae at the base of the damaged trichomes (Fig. 7D and E) and epicuticular wax flaking (Fig. 7C and F). These changes were observed in all monitored sites.

Cell death detection

The test for cell death was positive for all monitored species. In *M. alpigena*, at site 4, damage was observed in nonglandular trichomes, which were strongly stained by Evans Blue (Fig. 8A).

In *E. erythropappus*, only the individuals at site 2 had their cells stained by Evans Blue. This species showed a moderate group of stomatal cells weakly stained by the reagent (Fig. 8B).

In *B. variabilis* the test was positive for sites 1 (Fig. 8C and D) and 5 (Fig. 8E and F). The major reactions were observed in the stomata, at both sites.

It was not possible to perform the collection for cell death test in site 3 individuals due to the previously mentioned wildfire that occurred in the PEI.

Discussion

The species evaluated in this study did not show any visual symptoms, even though they had accumulated the pollutant and presented damage at the microscopic level, as verified by De Temmerman et al. (2004), Jha et al. (2009), and Mondal (2017).

In the present study, *Myrceugenia alpigena* accumulated an average fluoride content of 25.2 µg g^{-1}, followed by *Byrsonima variabilis* with 13.2 µg g^{-1} and 10.5 µg g^{-1} for *Eremanthus erythropappus*. The phytotoxicity of fluoride depends on the stage of leaf development, genetic susceptibility of the evaluated species, and concentration of the pollutant in the atmosphere (Treshow and Anderson 1989; Weinstein and Davison 2004). Treshow and Anderson (1989) suggested that sensitive plants show visual damage when the fluoride

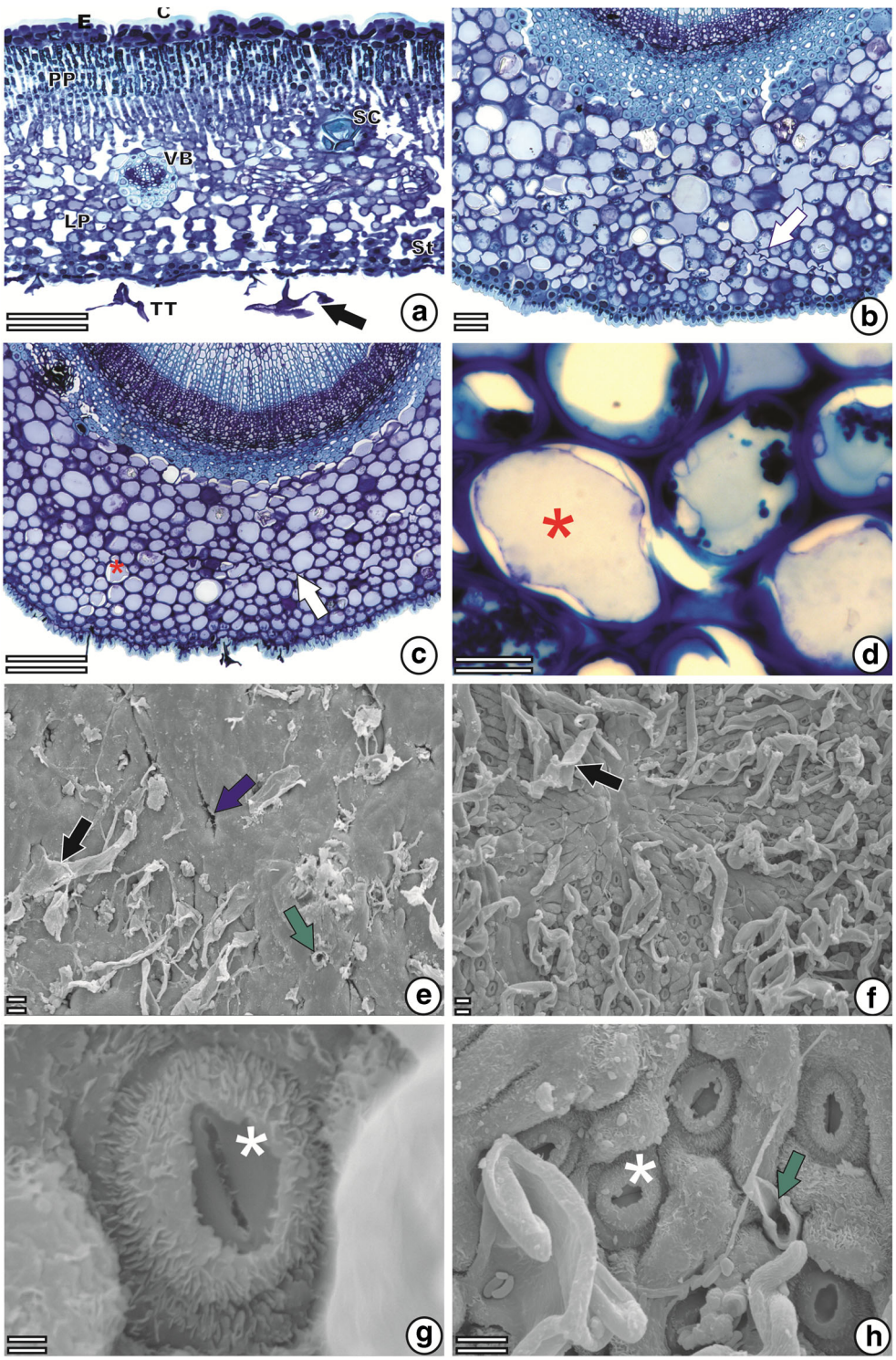

Fig. 5 Leaf blade of *Myrceugenia alpigena* without visual symptoms, monitored at Parque Estadual do Itacolomi (PEI). (A, B, C, and D) Light microscopy, in cross section. (E, F, G, and H). Scanning electron microscopy. (E) Adaxial surface. (F, G, H) Abaxial surface. (A, C, E, G) Site 3. (B, D, F, H) Site 4. Black arrows, damaged nonglandular trichome; white arrows, cells with altered shape; green arrows, broken trichome base; blue arrow, furrows formation; red asterisk, protoplast retraction; white asterisk, stoma with damaged ledge. C Cuticle. E Epidermis. PP, palisade parenchyma. SC, secretory cavity. VB, vascular bundle. LP, spongy parenchyma. St, stoma. TT, nonglandular trichome. Scales: (A) 100 μm. (B, C) 50 μm. (E, D, F) 20 μm. (G) 2 μm. (H) 10 μm

concentration in the plant is higher than 30 μg g^{-1} of dry matter. However, Oliva et al. (2005) detected chloroses and necrosis in grasses with foliar levels of fluoride between 4.7 and 27 μg g^{-1}, while for *Lolium multiflorum*, even at high concentrations of fluoride (180 μg g^{-1}), no visual damage was verified (Mesquita et al. 2011). This shows that the species susceptibility variation is not related to a fluoride concentration limit, but to the specific response of each organism to the pollutant. This was observed in the present study, in which the monitored species did not show visual symptoms, but showed considerable fluoride levels and anatomical changes.

Sites 3 and 4 stood out in the accumulation of fluoride in individuals of *M. alpigena*. This result is related to the fact that

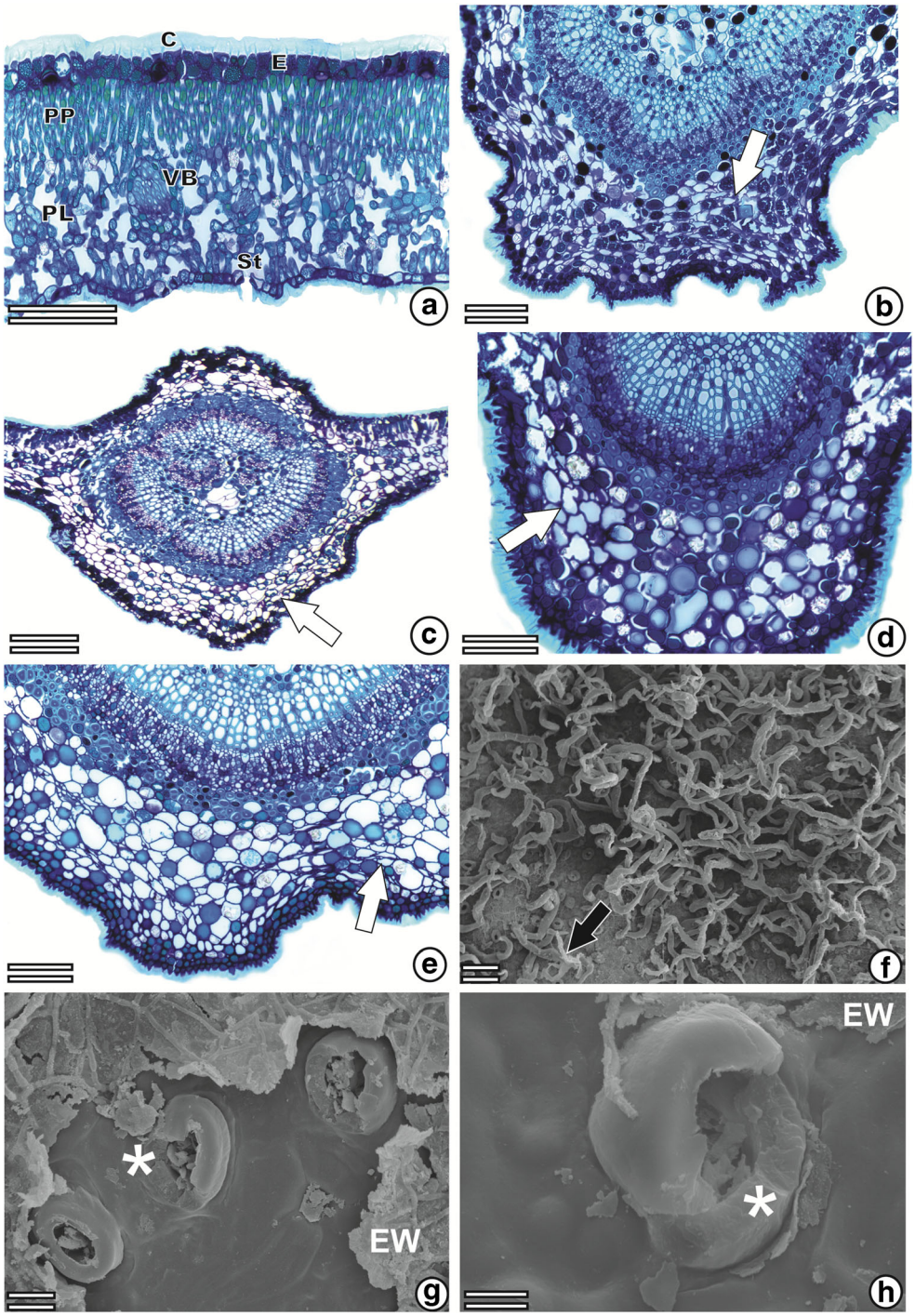

Fig. 6 Leaf blades of *Byrsonima variabilis*, without visual symptoms, monitored at Parque Estadual do Itacolomi (PEI). (A, B, C, D, and E) Light microscopy, in cross section. (F, G, and H) Scanning electron microscopy—abaxial surface. (A, B, G) Site 1. (C) Site 3. (D, F, H) Site 4. White arrows, cells with altered shape; black arrows, flaccid trichomes; white asterisk, stomata with broken ledges. EW, epicuticular wax flaking; C, cuticle. E, epidermis. PP, palisade parenchyma. VB, vascular bundle. PL, spongy parenchyma. St, stoma. (F, G, H) Abaxial surface. Scales: (A, B, D, E, F) 100 μm. (C) 200 μm. (G) 20 μm. (H) 10 μm

these sites are the closest to the emitting source among the sites inside the park, in addition to site 3 presenting a higher altitude and strong incidence of wind, which facilitates the arrival of pollutants to the plants, exposing them to wind currents from the smelter. Louback et al. (2016), in a study carried out in this same environmental preservation area, also found through active biomonitoring that the fluoride emission is reaching the PEI, mainly in locations closer to the smelter; however, the authors reported that the emitted fluoride is also reaching locations in the PEI that are farther from the polluting source.

The moderate accumulation of fluoride in *B. variabilis* may be related to the fact that this species has a thick cuticle and a dense cover of epicuticular wax, even over the stomata cells. Chaves et al. (2002), when comparing *Chloris gayana* and *Panicum maximum*, observed that the higher proportion of wax may be related to greater resistance to fluoride pollution in *C. gayana.* In *Eremanthus erythropappus*, in the present

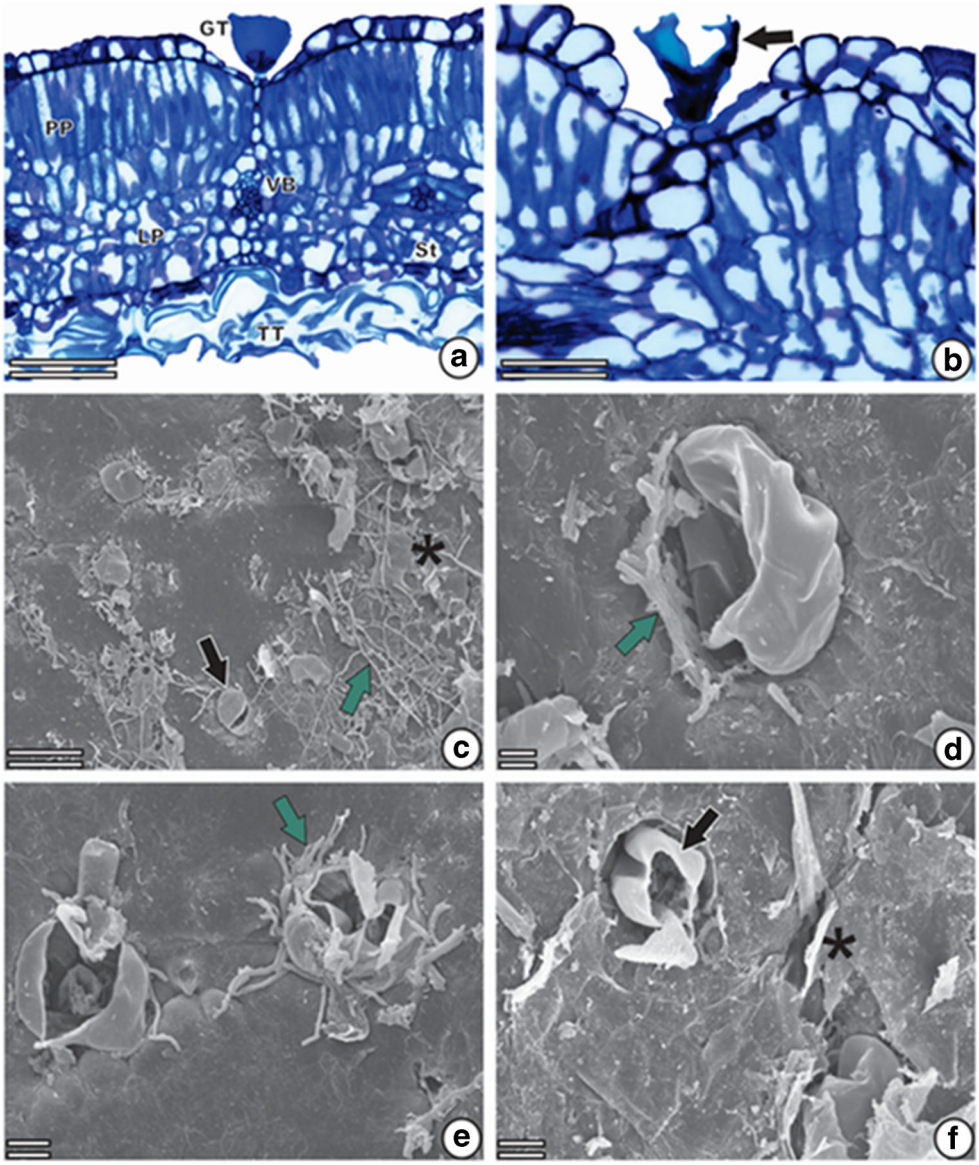

Fig. 7 Leaf blades of *Eremanthus erythropappus*, without visual symptoms, monitored at Parque Estadual do Itacolomi (PEI). (A, B) Light microscopy, in cross section. (C, F) Scanning electron microscopy—adaxial surface. (A, C) Site 1. (B, E) Site 3. (D) Site 2. (F) Site 4. Black arrows, damaged glandular trichomes; green arrows, proliferation of fungal hyphae; black asterisk, epicuticular wax flaking. GT, glandular trichome. PP, palisade parenchyma. VB, vascular bundle. LP, spongy parenchyma. St, stoma. TT, nonglandular trichome. (C, D, E, F) Adaxial surface. Scales: (A, C) 100 μm. (B) 50 μm. (D) 10 μm. (E, F) 20 μm

study, the high density of trichomes may have formed a barrier to the entrance of fluoride via stomata, as it was also observed by Chaves et al. (2002) in *Chloris gayana* and by Ribeiro (2008). Ribeiro (2008) evaluated four species from the Atlantic Forest and concluded that *E. erythropappus* has the ability to tolerate a high fluoride concentration while maintaining several physiological parameters unaltered. Thus, in this study, the lower fluoride content in *B. variabilis* and *E. erythropappus* is probably related to the anatomical structure of these species, which can provide a greater protection to the plant, by reducing the entry of pollutants into the leaf.

In the Evans Blue test, cell groups with altered membranes were observed, indicating that there was cell death in leaf regions of the three monitored species. This test is an important prognosis for cell death detection, even when injuries are not visualized (Faoro and Iriti 2005; Louback et al. 2016). It is known that the gaseous fluoride penetrates plants through stomata (Pita-Barbosa et al. 2009). Thus, in the present study, dead cells were observed close to these structures, indicating that cell death occurred due to the pollutant's entry (Gerosa et al. 2009; Alves et al. 2011), and that, consequently, with its accumulation inside the leaf, other tissues will be affected. Anjos et al. (2018) studied the effects of fluoride in simulated rain on the species *Spondias purpurea* and found that fluoride caused epidermal necrosis in this species, facilitated by absorption through stomata, and that after absorption of the pollutant, the damage progressed to the leaf mesophyll, promoting injuries in that region, leading to a total collapse of the mesophyll cells.

The three species monitored in the PEI showed micromorphological damage in their leaves. *M. alpigena* and *B. variabilis* showed more severe damage to trichomes and

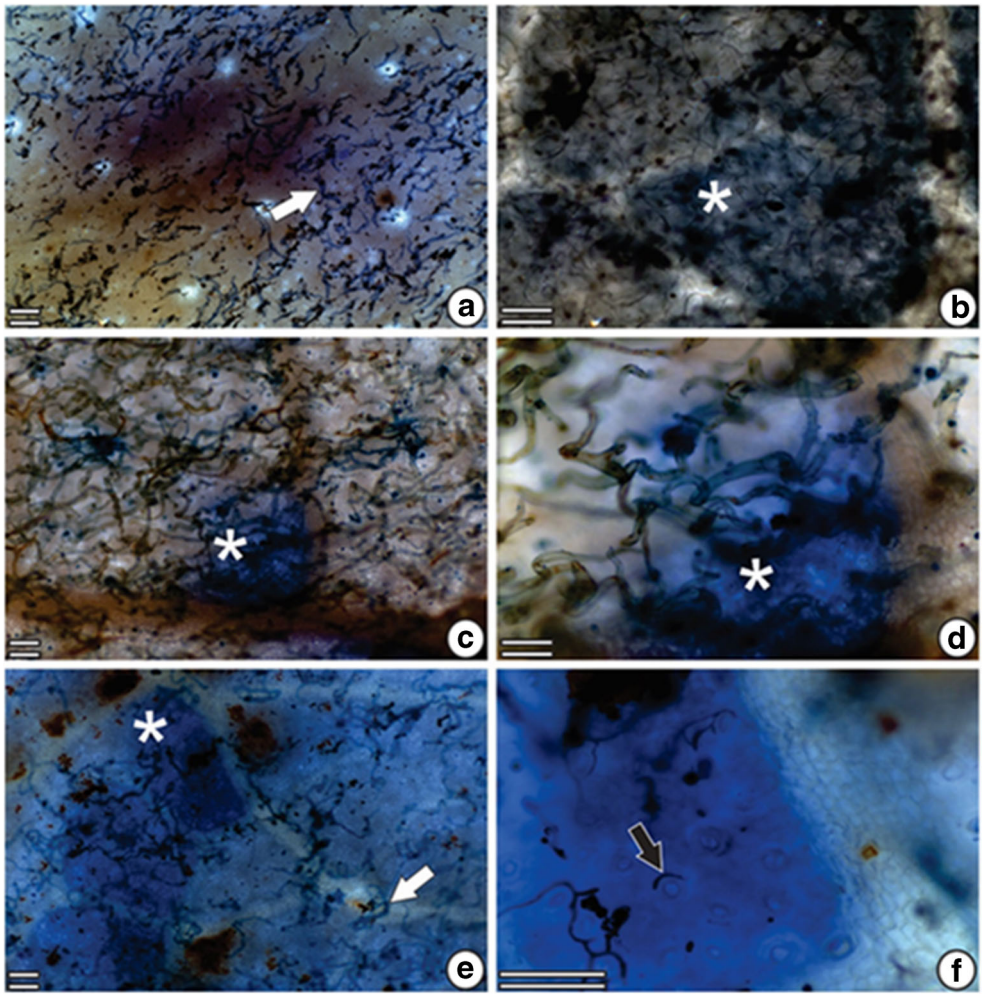

Fig. 8 Cell death in leaves of plants at Parque Estadual do Itacolomi (PEI) exposed to emissions from the smelter. Histochemical test with Evans Blue, in diaphanization. (A) Site 4, *M. alpigena*. (B) Site 2, *E. erythropappus*. (C, D) Site 1, *B. variabilis*. (E, F) Site 5, *B. variabilis*. White arrow, nonglandular trichomes stained by Evans Blue; white asterisk, group of dead cells; black arrow, stomata stained blue. Scales: (A, C, E) 150 μm. (B, D, F) 100 μm

stomata. Damage occurrence, mainly associated with stomata in *M. alpigena* and *B. variabilis*, has also been reported in other species (Chaves et al. 2002; Sant'Anna-Santos and Azevedo 2007; Pita-Barbosa et al. 2009; Cai et al. 2016; Sant'Anna-Santos et al. 2019), which is due to the fact that stomata are the main entry route for fluoride. In *Eremanthus erythropappus,* the micromorphological damages were more intense in the glandular trichomes that presented proliferation of fungal hyphae. The appearance of fungal hyphae has been observed previously in plants that were exposed in the PEI (Louback et al. 2016), and also in experiments conducted in a greenhouse, with simulated fluoride fog (Sant'Anna-Santos and Azevedo 2007; Sant'Anna-Santos et al. 2014; Anjos et al. 2018). The invasion of pathogens is related to the epicuticular wax flaking, which can facilitate the entry of fluoride into the epidermis and, secondarily, allow the invasion of pathogens (Pascholati and Leite 1995; Pozza et al. 2004).

Both in passive and active biomonitoring in the PEI, the monitored plants showed anatomical changes. The species monitored in our research showed protoplast retractions and changes in the shape of some cells; these damages were also reported by Louback et al. (2016) in exposed plants at the park. Thus, it is assumed that fluoride interacts with membrane components, changing its permeability, the lipid matrix, and interfering with its metabolic function and selectivity, which can lead to cell death (Fornasiero 2001; Kamaluddin and Zwiazek 2003; Weinstein and Davison 2003; Oliva et al. 2005), as verified in the present study. The interaction of fluoride with cells has been verified in several studies, in which the authors diagnosed damage to the cell structure in species that were exposed to the pollutant, such as deformities in the cell wall, increased sinuosity of the wall, protoplast retraction, and loss of turgidity. In some experiments, these cellular damages led to the formation of generalized necrosis and cell plasmolysis (Louback et al. 2016; Anjos et al. 2018; Rodrigues et al. 2018a; Sant'Anna-Santos et al. 2019; Rodrigues et al. 2020a, 2020b).

The light microscopy data corroborated the data found by scanning electron microscopy and the histochemical test for cell death, allowing us to state that the monitored species showed significant microscopic changes in response to fluoride, even though no visible injuries occurred.

Conclusions

The responses obtained through passive monitoring at the PEI lead us to conclude that the emissions from the aluminum smelter affect the native vegetation of this environmental conservation area. In addition, the greater accumulation of fluoride in *M. alpigena* and its broader diversity of symptoms, with considerable microscopic damage if compared to the other monitored species, enhances the use of this species in the monitoring of environments polluted by fluoride. It is worth noting, however, that analyses in a controlled environment are necessary in order to confirm the damage described in the field.

The study of the impact caused by the emission of fluoride on plants contributes to the understanding of abiotic factors that affect the species of the PEI, which alter communities and ecosystems, thus increasing human awareness of the effects of air pollution. The knowledge of the effects of fluoride on these native species of the PEI is of great importance, since the use of these species in environmental pollution biomonitoring programs can contribute to the preservation of the plants present in this park.

Acknowledgments The authors would like to thank CAPES (Coordenação de Aperfeiçoamento de Pessoal de Nível Superior) - Finance code 001 for the scholarship granted to Thamires Fernanda Gomes. L. C. Silva thanks the Conselho Nacional de Desenvolvimento Científico e Tecnológico (CNPq) for the Research Productivity Scholarship 309308/2018-6. We also thank the direction of the Parque Estadual do Itacolomi – MG, for the free access granted to us, "Laboratório de Anatomia Vegetal" and "Núcleo de Microscopia e Microanálise" of "Universidade Federal de Viçosa".

Authors' contributions - Thamires Fernanda Gomes participated in the research planning, field data and material collection, laboratory analysis and interpretation of the data obtained, and writing of the manuscript.

- Ademir Martins Lima participated in the data interpretation, writing, and revision of the manuscript.

- Ana Paula Pires Marques participated in the laboratory analysis and interpretation of the data obtained and writing of the manuscript.

- Luzimar Campos da Silva, research's advisor, oriented the research planning and the field data and material collection, supported the laboratory analysis and interpretation of the data obtained, and participated in the writing and revision of the manuscript.

Funding Coordenação de Aperfeiçoamento de Pessoal de Nível Superior (CAPES - Finance code 001) granted a scholarship to Thamires Fernanda Gomes during the research development. Conselho Nacional de Desenvolvimento Científico e Tecnológico (CNPq) granted the Research Productivity Scholarship 309308/2018-6.

Data availability The datasets used and/or analyzed during the current study are available from the corresponding author on reasonable request.

Declarations

Competing interests The authors declare no competing interests.

Ethics approval and consent to participate Not applicable.

Consent for publication Not applicable.

References

Ahmad MN, VandenBerg LJL, Shah HU, Masood T, Büker P, Emberson L, Ashmore M (2012) Hydrogen fluoride damage to vegetation from peri-urban brick kilns in Asia: a growing but unrecognised problem? Environ Pollut 162:319–324. https://doi.org/10.1016/j.envpol.2011.11.017

Alves ES, Moura BB, Pedroso ANV, Tresmondi F, Domingos M (2011) The efficiency of tobacco Bel-W3 and native species for ozone biomonitoring in sub-tropical climate, as revealed by histocytochemical techniques. Environ Pollut 159:3309–3315. https://doi.org/10.1016/j.envpol.2011.08.043

Anjos TBO, Louback E, Azevedo AA, Silva LC (2018) Sensibility of *Spondias purpurea* L. (Anacardiaceae) exposed to fluoride-simulated fog. Ecol Indic 90:154–163. https://doi.org/10.1016/j.ecolind.2018.03.005

Arndt U, Flores F, Weinstein LH (1995) Fluoride effects on plants, diagnose of injury in the vegetation of Brazil. Universidade Federal do Rio Grande do Sul, Porto Alegre, p 155

Assis CM, Silveira IL, Anizelli RCM (2003) Automonitoramento da qualidade do ar em Ouro Preto/MG. In: Congresso Interamericano de Qualidade do Ar, 3, Canoas. Anais Porto Alegre, AIDIS, ABES. 1 CD-ROM (in Portuguese, with English abstract).

Associação Brasileira do Alumínio – ABAL (Brasilian Aluminum Association) (2011) http://www.abal.org.br/estatisticas/nacionais/ (accessed on September 2020).

Baunthiyal M, Ranghar S (2014) Physiological and biochemical responses of plants under fluoride stress: an overview. Fluoride 47:287–293

Cai H, Dong Y, Li Y, Li D, Peng C, Zhang Z, Wan X (2016) Physiological and cellular responses to fluoride stress in tea (*Camellia sinensis*) leaves. Acta Physiol Plant 38:144. https://doi.org/10.1007/s11738-016-2156-0

Chaves ALF, Silva EAM, Azevedo AA, Cano MAO, Matsuoka K (2002) Ação do flúor dissolvido em chuva simulada sobre a estrutura foliar de *Panicum maximum* jacq. (colonião) e *Chloris gayana* kunth. (capim-rhodes)-Poaceae. Acta Bot Bras 16:395–406. https://doi.org/10.1590/S0102-33062002000400003

Coser TS, Paula CC, Wendt T (2010) Bromeliaceae Juss. nos campos rupestres do Parque Estadual do Itacolomi, Minas Gerais, Brasil. Rodriguésia 61:261–280. https://doi.org/10.1590/2175-7860201061209

Davison AW, Weinstein LH (2006) Some problems relating to fluorides in the environment: effects on plants and animals. In: Tressaud, A. (Ed.). Fluorine Environ Atmos Chem, Emiss Lithosph 1:251–298. https://doi.org/10.1016/S1872-0358(06)01008-6

Divan Junior AM, Oliva MA, Martinez CA, Cambraia J (2007) Effects of fluoride emissions on two tropical grasses: *Chloris gayana* and *Panicum maximum* cv. Colonião. Ecotoxicol Environ Saf 67:247–253. https://doi.org/10.1016/j.ecoenv.2006.06.002

Divan Junior AM, Oliva MA, Ferreira FA (2008) Dispersal pattern of airborne emissions from an aluminium smelter in Ouro Preto, Brazil, as expressed by foliar fluoride accumulation in eight plant species. Ecol Indic 8:454–461. https://doi.org/10.1016/j.ecolind.2007.04.008

Faoro F, Iriti M (2005) Cell death behind invisible symptoms: early diagnosis of ozone injury. Biol Plant 49:585–592. https://doi.org/10.1007/s10535-005-0053-2

Ferreira DF (2011) Sisvar: a computer statistical analysis system. Ciência Agrotecnol 35:1039–1042. https://doi.org/10.1590/S1413-70542011000600001

Fialho RC (1997) Acumulação foliar de fluoretos e seu significado ecológico em espécies arbóreas da Mata Atlântica, Cubatão, SP. 100 f. Dissertação (Mestrado) - Instituto de Biociências, Universidade de São Paulo, São Paulo.

Fordyce FM, Vrana K, Zhovinsky E, Povoroznuk V, Toth G, Hope BC, Iljinsky U, Baker J (2007) A health risk assessment for fluoride in Central Europe. Environ Geochem Health 29:83–102. https://doi.org/10.1007/s10653-006-9076-7

Fornasiero RB (2001) Phytotoxic effects of fluorides. Plant Sci 161:979–985. https://doi.org/10.1016/S0168-9452(01)00499-X

Fornasiero RB (2003) Fluorides effects on *Hypericum perforatum* plants: first field observations. Plant Sci 165:507–513. https://doi.org/10.1016/S0168-9452(03)00205-X

Fuge R (2019) Fluorine in the environment: a review of its sources and geochemistry. Appl Geochem 100:393–406. https://doi.org/10.1016/j.apgeochem.2018.12.016

Gaff DF, Okong'o-ogola O (1971) The use of non-permeating pigments for testing the survival of cells. J Exp Bot 22:756–758. https://doi.org/10.1093/jxb/22.3.756

Gerosa G, Marzuoli R, Rossini M, Panigada C, Meroni M, Colombo R, Faoro F, Iriti M (2009) A flux-based assessment of the effects of ozone on foliar injury, photosynthesis, and yield of bean (*Phaseolus vulgaris* L. cv. Borlotto Nano Lingua di Fuoco) in open-top chambers. Environ Pollut 157:1727–1736. https://doi.org/10.1016/j.envpol.2008.06.028

Gerrits PO (1964) The application of glycol methacrylate histotechnology: some ground principles. Leica GmbH, Germany

Gorelova SV, Frontasyeva MV (2017) The use of higher plants in biomonitoring and environmental bioremediation. In: Ansari A, Gill S, Gill R, Lanza RG, Newman L (eds) Phytoremediation. Springer, Cham. https://doi.org/10.1007/978-3-319-52381-1_5

Gupta GP, Kulshrestha U (2016) Biomonitoring and remediation by plants. In: Kulshrestha U, Saxena P (eds) Plant Responses to Air Pollution. Springer, Singapore. https://doi.org/10.1007/978-981-10-1201-3_11

Hong X, Liang H, Chen Y, Liu Y, Shi Y (2018) Distribution of fluorine in the surface dust of Wuda coal base, Inner Mongolia of Northern China. J Geochem Explor 188:390–397. https://doi.org/10.1016/j.gexplo.2018.02.012

Jha SK, Nayak AK, Sharma YK (2009) Fluoride toxicity effects in onion (*Allium cepa* L) grown in contaminated soils. Chemosphere 76:353–356. https://doi.org/10.1016/j.chemosphere.2009.03.044

Kamaluddin M, Zwiazek JJ (2003) Fluoride inhibits root water transport and affects leaf expansion and gas exchange in aspen (*Populus tremuloides*) seedlings. Physiol Plant 117:368–375. https://doi.org/10.1034/j.1399-3054.2003.00040.x

Karnovsky MJ (1965) A formaldehyfr-glutaraldehyde fixative of high osmolality for use in electron microscopy. J Cell Biol 27:137–138. https://doi.org/10.1038/srep27790

Kato T, Sato N, Hayama S, Yamabuki T, Ito T, Miyamoto M, Kondo S, Nakamura Y, Daigo Y (2007) Activation of Holliday junction-recognizing protein involved in the chromosomal stability and immortality of cancer cells. Cancer Res 67:8544–8553. https://doi.org/10.1158/0008-5472.CAN-07-1307

Klumpp A, Domingos M, Klumpp G (1996) Assessment of the vegetation risk by fluoride emissions from fertiliser industries at Cubatao, Brazil. Sci Total Environ 192:219–228. https://doi.org/10.1016/S0048-9697(96)05298-9

Klumpp A, Domingos M, Moraes RM, Klumpp G (1998) Effects of complex air pollution on tree species of the Atlantic rain forest near Cubatão, Brazil. Chemosphere 36:989–994. https://doi.org/10.1016/S0045-6535(97)10160-6

Klumpp A, Ansel W, Klumpp G, Fomin A (2001) Um novo conceito de monitoramento e comunicação ambiental: a rede européia para a avaliação da qualidade do ar usando plantas bioindicadoras (EuroBionet). Rev Bras Bot 24:511–518. https://doi.org/10.1590/S0100-84042001000500005

Koslowski TT (1980) Impacts of air pollution on forest ecosystems. Bioscience 30:88–93. https://doi.org/10.2307/1307913

Li M, Li C, Zhang M (2018) Exploring the spatial spillover effects of industrialization and urbanization factors on pollutants emissions in China's Huang-Huai-Hai region. J Clean Prod 195:154–162. https://doi.org/10.1016/j.jclepro.2018.05.186

Louback E, Pereira TAR, Souza SR, Oliveira JA, Silva LC (2016) Vegetation damage in the vicinity of an aluminum smelter in Brazil. Ecol Indic 67:193–203. https://doi.org/10.1016/j.ecolind.2016.02.044

Matthews RA, Buikema AL, Cairns JJ, Rodgers JJH (1982) Biological monitoring part IIA: receiving system functional methods relationships, and indices. Wat Resea 16:129–139. https://doi.org/10.1016/0043-1354(82)90102-6

Mesquita GL, Tanaka FAO, Cantarella H, Mattos D (2011) Atmospheric absorption of fluoride by cultivated species. Leaf structural changes and plant growth. Water Air Soil Pollut 219:143–156. https://doi.org/10.1007/s11270-010-0694-4

Messias MCTB, Sousa HC, Scalon VR, Roschel MB, Cândido ES, Fujaco MAG (2017) Phanerogamic flora and vegetation of Itacolomi State Park, Minas Gerais, Brazil. Biota Neotrop 17:1–38. https://doi.org/10.1590/1676-0611-bn-2016-0236

Mondal NK (2017) Effect of fluoride on photosynthesis, growth and accumulation of four widely cultivated rice (*Oryza sativa* L.) varieties in India. Ecotox Environ Safety 144:36–44. https://doi.org/10.1016/j.ecoenv.2017.06.009

Mukherjee A, Pandey B, Agrawal SB, Agrawal M (2019) Responses of tropical and subtropical plants to air pollution. In: Garkoti S, Van Bloem S, Fulé P, Semwal R (eds) Tropical Ecosystems: Structure, Functions and Challenges in the Face of Global Change. Springer, Singapore. https://doi.org/10.1007/978-981-13-8249-9_7

O'Brien TP, McCully ME (1981) The study of plants structure principles and select methods. Termarcarphi Pty. Ltda, Melbourne, p 45

Oliva MA, Figueiredo GDE, Nees S, Stapf N (2005) Gramíneas bioindicadoras da presença de flúor em regiões tropicais. Pesqui Agropecuária Bras 1:389–397. https://doi.org/10.1590/S0100-84042005000200017

Panda D (2015) Fluoride toxicity stress: physiological and biochemical consequences on plants. Int J Bioresour Environ Agric Sci 1:70–84

Pascholati SF, Leite B (1995) Hospedeiros: mecanismos de resistência. In: Bergamin Filho A, Kimati H, Amorin L (eds) Manual de Fitopatologia – princípios e conceitos. Ceres, São Paulo, pp 417–453

Peron MV (1989) Listagem preliminar da flora fanerogâmica dos Campos Rupestres do Parque Estadual do Itacolomi, Ouro Preto/Mariana, MG. Rodriguésia 41:63–69. https://doi.org/10.1590/2175-78601989416705

Pita-Barbosa A, Sant'Anna-santos BF, Silva KLF, Azevedo AA, Rocha DI (2009) Efeitos fitotóxicos do fluoreto na morfoanatomia foliar de *Brachiaria brizantha* (Hochst. ex A. Rich.) Stapf e Brachiaria decumbens Stapf (Poaceae). Acta Bot Bras 23:1027–1033. https://doi.org/10.1590/S0102-33062009000400012

Pozza AAA, Alves E, Pozza EA, Carvalho JG, Montanari M, Guimarães PTG, Santos DM (2004) Efeito do silício no controle da cercosporiose em três variedades de cafeeiro. Fitopatol Bras 29:185–188. https://doi.org/10.1590/S0100-41582004000200010

Ribeiro SFC (2008) Efeitos da aplicação de flúor sobre os processos fotossintéticos em três espécies lenhosas e nativas da região de Ouro Preto – MG. 63 f. Dissertação (Mestrado em Fisiologia Vegetal) – Universidade Federal de Viçosa, Viçosa, MG

Rodrigues AA, Vasconcelos-Filho SC, Mendes GC, Rehn LS, Rodrigues DA, Rodrigues CL, Müller C (2017) Fluoride in simulated rain affects the morphoanatomy and physiology of *Eugenia dysenterica* (Mart.) DC. Ecol Indic 82:189–195. https://doi.org/10.1016/j.ecolind.2017.07.005

Rodrigues AA, Vasconcelos-Filho SC, Müller C, Rodrigues DA, Mendes GC, Rehn LS, Costa AC, Vital RG, Sales JF (2018a) *Sapindus saponaria* bioindicator potential concerning potassium fluoride exposure by simulated rainfall: anatomical and physiological traits. Ecol Indic 89:552–558. https://doi.org/10.1016/j.ecolind.2018.02.043

Rodrigues DA, Vasconcelos-Filho SC, Rodrigues AA, Müller C, Farnese FS, Costa AC, Teles EMG, Rodrigues CL (2018b) *Byrsonima basiloba* as a bioindicator of simulated air pollutants: morphoanatomical and physiological changes in response to potassium fluoride. Ecol Indic 89:301–308. https://doi.org/10.1016/j.ecolind.2018.02.019

Rodrigues DA, de Fátima SJ, Vasconcelos-Filho SC, Rodrigues AA, Costa AC, Rodrigues CL, Lima FH, Müller CS (2020a) *Spondias mombin*, a potential bioindicator of potassium fluoride pollution. Ecol Indic 114:106314. https://doi.org/10.1016/j.ecolind.2020.106314

Rodrigues DA, de Fátima SJ, Vasconcelos-Filho SC, Rodrigues AA, Teles EMG, Costa AC, Reis EL, de Carvalho Silva TA, Müller C (2020b) Bioindicator potential of Ricinus communis to simulated rainfall containing potassium fluoride. PeerJ 8:9445. https://doi.org/10.7717/peerj.9445

Romero R, Nakajima JN (1999) Espécies endêmicas do Parque Nacional da Serra da Canastra, Minas Gerais. Rev Bras Bot 22:259–265. https://doi.org/10.1590/S0100-84041999000500006

Sant'Anna-Santos BF, Azevedo AA (2007) Aspectos morfoanatômicos da fitotoxidez do flúor em duas espécies arbóreas tropicais. Rev Bras Biociências 5:48–50

Sant'Anna-Santos BF, Azevedo AA (2010) Toxicidade e acúmulo de flúor em hortaliças nas adjacências de uma fábrica de alumínio. Acta Bot Bras 24:952–963. https://doi.org/10.1590/S0102-33062010000400010

Sant'Anna-Santos BF, Azevedo AA, Silva LC, Oliva MA (2012) Diagnostic and prognostic characteristics of phytotoxicity caused by fluoride on *Spondias dulcis* Forst. F. (Anacardiaceae). An Acad Bras Cienc 84:689–702. https://doi.org/10.1590/S0001-37652012005000048

Sant'Anna-Santos BF, Azevedo AA, Alves TG, Campos NV, Oliva MA, Valente VMM (2014) Effects of emissions from an aluminium smelter in a tree tropical species sensitive to fluoride. Water Air Soil Pollut 225:1817. https://doi.org/10.1007/s11270-013-1817-5

Sant'Anna-Santos BF, Azevedo AA, Oliva MA, Campos NV, Gomes MP (2019) What precedes fluoride-response symptomatology: microscopic or physiological damage? Ecol Indic 107:105–560. https://doi.org/10.1016/j.ecolind.2019.105560

Sharma R, Kaur R (2018) Insights into fluoride-induced oxidative stress and antioxidant defences in plants. Acta Physiol Plant 40:10–181. https://doi.org/10.1007/s11738-018-2754-0

Silva LC, Azevedo AA, Silva EAM, Oliva MA (2000) Flúor em chuva simulada: sintomatologia e efeitos sobre a estrutura foliar e o crescimento de plantas arbóreas. Rev Bras Bot 23:385–393. https://doi.org/10.1590/S0100-84042000000400004

Temmerman L, Bell JNB, Garrec JP, Klumpp A, Krause GHM, Tonneijck AEG (2004) Biomonitoring of air pollutants with plants – considerations for the future. In: Klumpp A, Ansel W, Klumpp G (eds) Urban air pollution, bioindication and environmental awareness. Cuvillier Verlag, Göttingen, pp 337–373

Treshow M, Anderson FK (1989) Plant stress from air pollution. John Wiley and Sons Ltd, Chichester

Weinstein LH, Davison AW (2003) Native plant species suitable as bioindicators and biomonitors for airborne fluoride. Environ Pollut 125:3–11. https://doi.org/10.1016/S0269-7491(03)00090-3

Weinstein LH, Davison AW (2004) Fluorides in the environment: effects on plants and animals. CABI Publishing, Oxford, p 287

Weinstein LH, Hansen KS (1988) Relative susceptibilities of Brazilian vegetation to airborne fluoride. Pesq Agropec 23(1125-11):37

Weinstein LH, Laurence JA, Mandl RH, Waelti K (1990) Use of native and cultivated plants as bioindicators and biomonitors of pollution damage. Am Soc Test Mater Philadelphia. https://doi.org/10.1520/STP19057S

Yalaltdinova A, Kim J, Baranovskaya N, Rikhvanov L (2018) *Populus nigra* L. as a bioindicator of atmospheric trace element pollution and potential toxic impacts on human and ecosystem. Ecol Indic 95:974–983. https://doi.org/10.1016/j.ecolind.2017.06.021

Yepu L, Shengli W, Prete D, Suyin X, Zhongren X, Fei Z, Qian Z (2017) Accumulation and interaction of fluoride and cadmium in the soil-wheat plant system from the wastewater irrigated soil of an oasis region in northwest China. Sci Total Environ 595:344–351. https://doi.org/10.1016/j.scitotenv.2017.03.288